Porous scaffolds for bone regeneration

Abbasi, Naghmeh; Hamlet, Stephen; Love, Robert M.; Nguyen, Nam Trung

Published in:
Journal of Science: Advanced Materials and Devices

DOI:
10.1016/j.jsamd.2020.01.007

Journal of Science: Advanced Materials and Devices 5 (2020) 1–9

Contents lists available at ScienceDirect

Journal of Science: Advanced Materials and Devices

journal homepage: www.elsevier.com/locate/jsamd

Review Article

Porous scaffolds for bone regeneration

Naghmeh Abbasi [a, b, **], Stephen Hamlet [a, b], Robert M. Love [a], Nam-Trung Nguyen [c, *]

[a] School of Dentistry and Oral Health, Griffith University, Gold Coast Campus, Southport, Queensland, 4215, Australia
[b] Menzies Health Institute Queensland, Griffith University, Gold Coast Campus, Southport, Queensland, 4215, Australia
[c] Queensland Micro- and Nanotechnology Centre, Griffith University, Nathan Campus, 170 Kessels Road, Queensland, 4111, Brisbane, Australia

ARTICLE INFO

Article history:
Received 26 November 2019
Received in revised form
30 January 2020
Accepted 30 January 2020
Available online 7 February 2020

Keywords:
Pore size
Pore geometry
Porosity
Tissue engineering
Biomaterials
Bone regeneration
Scaffold

ABSTRACT

Globally, bone fractures due to osteoporosis occur every 20 s in people aged over 50 years. The significant healthcare costs required to manage this problem are further exacerbated by the long healing times experienced with current treatment practices. Novel treatment approaches such as tissue engineering, is using biomaterial scaffolds to stimulate and guide the regeneration of damaged tissue that cannot heal spontaneously. Scaffolds provide a three-dimensional network that mimics the extra cellular micro-environment supporting the viability, attachment, growth and migration of cells whilst maintaining the structure of the regenerated tissue *in vivo*.

The osteogenic capability of the scaffold is influenced by the interconnections between the scaffold pores which facilitate cell distribution, integration with the host tissue and capillary ingrowth. Hence, the preparation of bone scaffolds with applicable pore size and interconnectivity is a significant issue in bone tissue engineering. To be effective however *in vivo*, the scaffold must also cope with the requirements for physiological mechanical loading. This review focuses on the relationship between the porosity and pore size of scaffolds and subsequent osteogenesis, vascularisation and scaffold degradation during bone regeneration.

1. Introduction

Tissue engineering techniques to produce biocompatible scaffolds populated with autogenous cells has recently been shown to be an ideal alternative method to provide bone substitutes [1]. Unlike many other tissues, minor bone tissue damage can regenerate by itself [2]. However, the bone's ability for self-repair of massive defects can be limited because of deficiencies in blood supply or in the presence of systemic disease [3]. Bone-lining cells are responsible for matrix preservation, mineralisation and resorption, and serve as precursors of osteoblasts [4]. However the penetration, proliferation, differentiation and migration abilities of these cells are affected by the size and geometry of the scaffold's pores and the degree of vascularisation [5].

Bone tissue engineering requires a suitable architecture for the porous scaffold. Sufficient porosity of suitable size and interconnections between the pores, provides an environment to promote cell infiltration, migration, vascularisation, nutrient and oxygen flow and removal of waste materials while being able to withstand external loading stresses [6]. The pore distribution and geometry of scaffold strongly influences cells ability to penetrate, proliferate and differentiate as well as the rate of scaffold degradation. The scaffold degradation rate needs to be compatible with the maturation and regeneration of new tissue after transplantation *in vivo* [7]. Therefore, materials of ultra-high molecular weight that do not degrade in the body have limited use as bone graft materials [8]. The products of the degradation process should also be non-toxic and not stimulate an inflammatory response [9]. As such the appropriate physical and chemical surface properties of the scaffold are an inherent requirement for promoting the attachment, infiltration, growth, proliferation and migration of cells [10].

2. Methods for the fabrication of porous scaffolds

A number of methods have been used to control the porosity of a scaffold (Fig. 1). The combination of the freeze-drying and leaching template techniques generates porous structures. In this method,

* Corresponding author. QLD Micro- and Nanotechnology Centre, Nathan campus, Griffith University, 170 Kessels Road QLD 4111, Australia.
** Corresponding author. School of Dentistry and Oral Health, Griffith University, Gold Coast Campus, QLD 4222, Australia.
E-mail addresses: naghmeh.abbasi@griffithuni.edu.au, naghme.k@gmail.com (N. Abbasi), s.hamlet@griffith.edu.au (S. Hamlet), r.love@griffith.edu.au (R.M. Love), nam-trung.nguyen@griffith.edu.au (N.-T. Nguyen).
Peer review under responsibility of Vietnam National University, Hanoi.

https://doi.org/10.1016/j.jsamd.2020.01.007

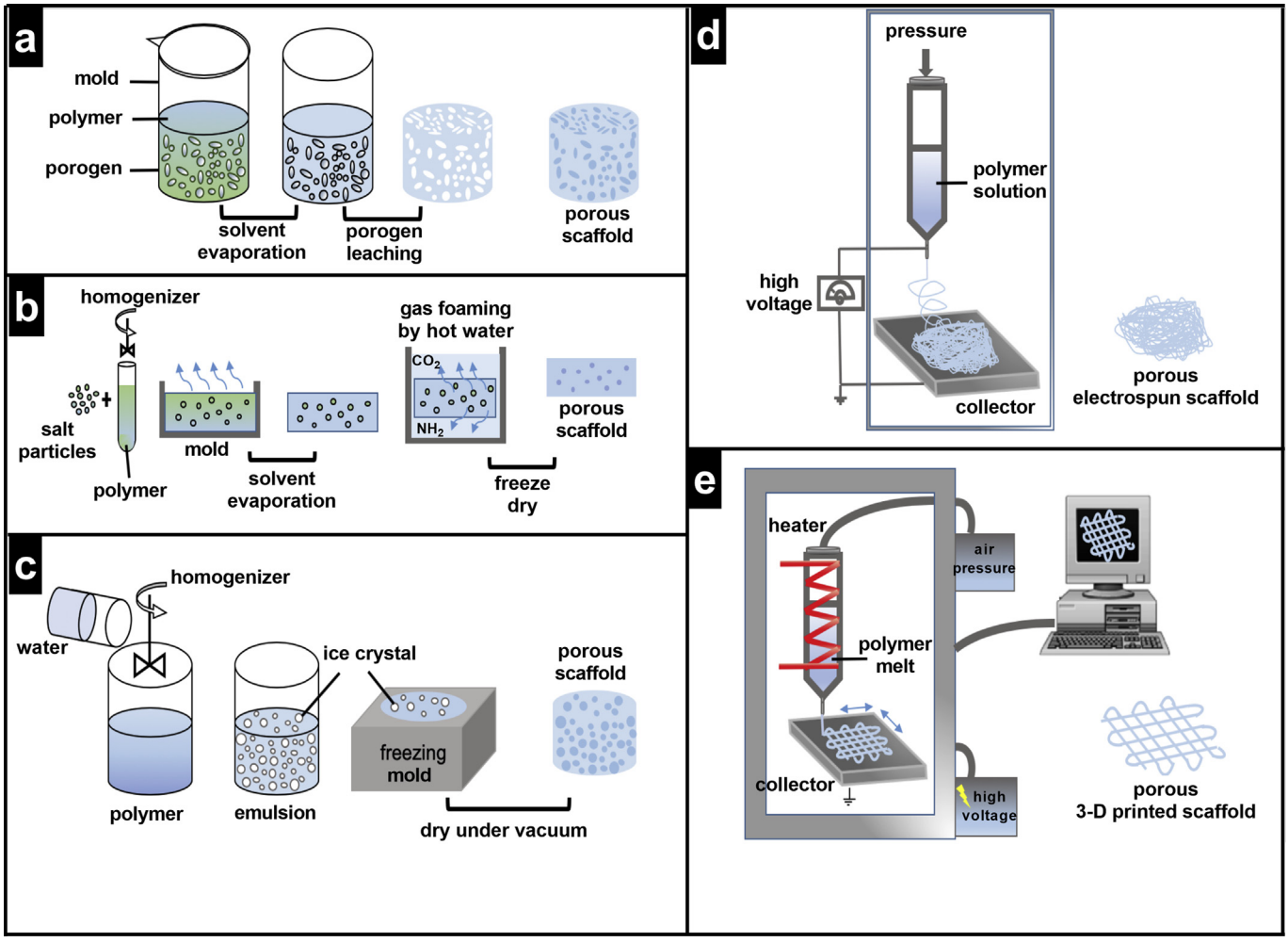

Fig. 1. Various porous scaffold fabrication techniques. (a) Porogen leaching, (b) Gas foaming, (c) Freeze-drying, (d) Solution electrospinning, (e) Melt electrowriting and 3-D printing.

the pore size can be adjusted by controlling the gap space of the leaching template, temperature changes and varying the density or the viscosity of the polymer solution concentration during freeze drying technique [11–13]. It is not yet clear whether scaffolds with uniform pore distribution and homogeneous size are more efficient in tissue regeneration than those with varying pore size distribution. Supercritical CO_2 foaming and melt processing is another method to produce porous scaffolds with different pore sizes. In this method, the molecular weight of the polymer component is changed, which affects the pore architecture [14].

Other fabrication methods for creating porous scaffolds in macroscale dimensions include rapid prototyping, immersion precipitation, freeze drying, salt leaching and laser sintering [15]. Scaffolds with high interconnectivity and heterogeneous (large and small) pores can be obtained by using melt mixing of the two polymers [16]. Of these methods, electrospinning method delivers fibres with nanometre dimensions because of the high surface-area-to-volume ratio, a property that is exploited to ensure a suitable surface for cell adhesion. The instability of the electrostatically drawn polymer causes the jet to whip about depositing the fibre randomly [17]. The formation of ordered structures by controlling fibre placement is one of the challenges of electrospinning. The charges of the electrospun fibres can produce a firmly compressed nonwoven mesh with very small pore sizes, which prevents cell infiltration [18]. Modified patterned stainless steel collectors or the use of cubic or circular holes as the template allow for the production of macroporous architecture scaffolds with an adequately large pore size to allow cell infiltration [19]. However, the direct melt electrowriting (MEW) technique is the most appropriate candidate for generating homogeneous porous biomaterials with a large ordered pore size (>100 μm). MEW can provide a suitable substrate to enable cells to penetrate sufficiently by controlling filament deposition on a collector resulting in customisable pore shapes with specific pore size [20].

The morphology of the scaffold is a key aspect that affects the migration of cells [21]. The key parameters to consider when optimising this scaffold morphology to create a scaffold with balanced biological and physical properties include the total porosity, pore morphology, pore size and pore distribution in the scaffold [22].

3. Role of porosity in bone engineering applications

3.1. Homogeneous pore size

The size of osteoblasts is on the order of 10–50 μm [23], however osteoblasts prefer larger pores (100–200 μm) for regenerating mineralised bone after implantation. This allows macrophages to infiltrate, eliminate bacteria and induce the infiltration of other cells involved in colonisation, migration and vascularisation *in vivo*

[24]. Whereas a smaller pore size (<100 μm) is associated with the formation of non-mineralised osteoid or fibrous tissue [24,25]. Early studies demonstrated significant bone formation in 800 μm scaffolds. Smaller pores were filled with fibroblasts while bone cells preferred to be located in larger pores suggesting a pore size of 800 μm was more appropriate to provide adequate space for cell ingrowth [26]. Similarly, Cheng et al. [27] using magnesium scaffolds with two pore sizes of 250 and 400 μm, showed that the larger pore size leads to greater formation of mature bone by promoting vascularisation. This is due to newly formed blood vessels which supply sufficient oxygen and nutrients for osteoblastic activity in the larger pores of implanted scaffolds which leads to the upregulation of osteopontin (OPN) and collagen type I and subsequent generation of bone mass [27].

Lim et al. however reported that pore sizes in the range of 200–350 μm was optimal for osteoblast proliferation whereas a larger pore size (500 μm) did not affect cell attachment [28]. Smaller pores are suitable for controlling cell aggregation and proliferation [29] however the exogenous hypoxic state associated with these scaffolds stimulates endothelial cell proliferation [30]. Also, proinflammatory cytokines such as tumour necrosis factor α and interleukin 6, 10, 12 and 13 are secreted at higher levels in larger pores and can trigger bone regeneration response [31].

In contrast to macropores, micropores provide a greater surface area, favourable protein adhesion and cell attachment on the scaffold *in vitro* [20]. O'Brien et al. suggested that the best pore size for initial cell adhesion was 95 μm *in vitro* [32]. Murphy et al. reported that a pore size of 100–325 μm was optimal for bone engineering scaffolds *in vitro* [33]. Previous studies have shown that although a pore size >50 μm (macropores) has beneficial effects on osteogenic quality, cell infiltration is restricted by small pore size *in-vitro*. Pore size <10 μm (micropore) creates a larger surface area that stimulates greater ion exchange and bone protein adsorption [34,35].

3.2. Heterogeneous pore size

Natural variation in bone density occurs in the axial direction of long bones, displaying a gradient in porous structure from cortical bone to cancellous bone [36]. This suggests bone implants made of porous gradient biomaterials that can mimic the properties of natural bone with a porosity-graded structure, may perform significantly better in bone regeneration applications. Boccaccio et al. (2016) showed a more porous layer imitated light spongy cancellous bone which had greater cell growth and transport of nutrients and waste in the highly porous region. Whereas, a compact and dense layer simulating the stiff cortical human bone was favourable for external mechanical loading [37]. Therefore, scaffolds with a gradient in porosity may be a good candidate for bone regeneration. According to Luca et al., gradient PCL scaffolds improved the osteogenic differentiation of human mesenchymal stem cells (MSCs) *in vitro* by increasing the calcium content and ALP activity because of the better supply of oxygen and nutrients in larger pores [38]. Sobral et al. evaluated cell-seeding efficiency of a human osteosarcoma cell in 3D poly (ε-caprolactone) scaffolds with two gradient pore sizes; 100–700–100 μm and 700–100–700 μm. The pore-size gradient scaffolds exhibited better seeding efficiency, which increased from about 35% in homogeneous scaffolds to about 70% in the gradient scaffolds under static culture conditions [39].

3.3. Pore geometry

Another feature that influences the rate of bone regeneration is the geometry of the porous scaffold [40]. Most scaffolds designed for tissue engineering have different pore morphologies as a result of the differing methods i.e. salt leaching, gas foaming, freeze drying, rapid prototyping (RP) and 3D printing techniques [12,41]. Differences in pore width and curvature of the surface have been shown to lead to variations in tissue morphology and growth rate. A high growth rate associated with higher curvature. In other words, more tissue is formed because of the smaller vertical spaces between the struts [42]. Similar results were reported with greater cell proliferation occurring at the short edges of rectangular pores than at the long edges [15,42].

Tissue formation favours concave surfaces compared with flat and convex regions. Concave surfaces provide room for cell alignment, whereas convex surfaces delay tissue growth [42], as there is greater cell stress and density of actin and myosin fibres in concave areas that advances the cells migration [43]. Larger pores have a larger perimeter and less curvature (Fig. 2) [42]. There are no experimental data to support the hypothesis that minimum cell stress increases bone regeneration. However, this hypothesis is based on the stability and equilibrium of the cells to minimise their energy on a minimum surface area [42,44]. This reflects the natural tendency of molecules to minimise their energy. Therefore, cells try to reduce their surface energy to the lowest possible level by reaching the most stable state on the corners of the pore to have more contact with other cells. At the corners of a pore, the small angle of struts provides a suitable environment for cells to interact and to minimise their residual energy, whereas cells at the pore centre have the highest level of energy and are in an unsteady state [45].

According to Van Bael et al., Ti_6Al_4V scaffolds with hexagonal pores showed the highest cell growth, and decreased with rectangular pores and decreased further with triangular pores (Fig. 3). The reason for these differences is the higher number of corners and the short distance between the two arches in the corners, particularly in hexagonal pores. This means that cell bridging occurs faster in hexagonal pores compared to rectangular and triangular pores whose struts are further apart. However, they found out the regulation of osteogenic differentiation of the cells was independent to their proliferation and ALP activity increased in triangular pores [46].

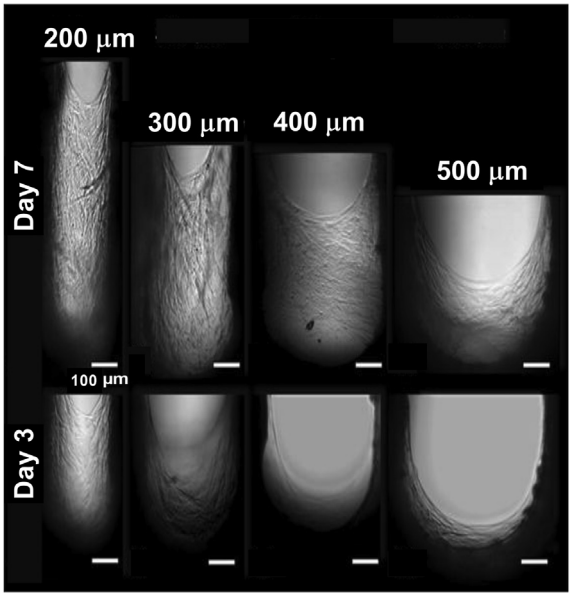

Fig. 2. Optical microscopy showing the tissue growing suspended in the open pore slots. Bottom: day 3. Top: day 7. Pore width 200, 300, 400, 500 μm from left to right. Image and caption are from Knychala et al. [42].

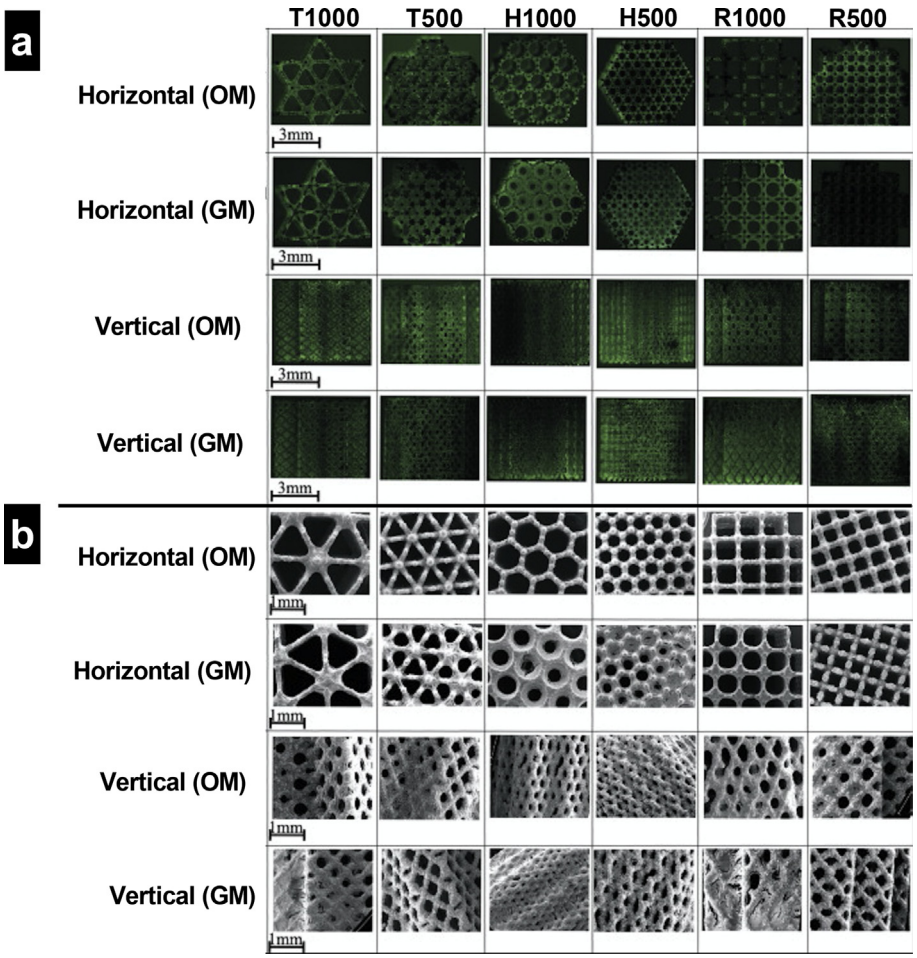

Fig. 3. (a) Representative images of live/dead staining; Green fluorescence indicates living cells. (b) SEM images in the horizontal and vertical plane of osteoprogenitor cells on the six porous Ti6Al4V scaffold designs for 14 days. SEM images revealed a difference in amount of pore occlusion between the different designs (T: triangular, H: hexagonal, R: rectangular) and culture media (OM: osteogenic medium or GM: growth medium). Image and caption are from Van Bael et al. [46].

Xu et al. reported that parallelogram and triangular shaped 3D-printed macroporous nagelschmidtite (NAGEL, $Ca_7Si_2P_2O_{16}$) bioceramic scaffolds exhibited greater proliferation than the square morphology. The parallelogram morphology had the highest ALP activity in the NAGEL scaffold compared with the other pore morphologies [47]. Yilgor et al. designed and constructed four complex structures of 3D printed porous PCL scaffold by changing the configuration of the deposited fibres within the architecture (basic, basic-offset, crossed and crossed-offset) (Fig. 4) [48]. Greater mesenchymal stem cells (MSCs) cell proliferation was observed for the basic offset scaffolds compared with higher cell differentiation and ALP activity in crossed scaffolds. These findings suggest that the basic-offset scaffolds (homogeneous structure) allowed cells to grow homogeneously because of the higher number of anchorage points. Interconnected struts created the angles, which differed from those in basic scaffolds and increased differentiation [48].

In a similar study, Yeo et al. fabricated various PCL−β-TCP (20 wt %) scaffolds with a square pore shape, but with five pore sizes of different offset values (0%, 25%, 50%, 75% and 100%). They found superior cell differentiation and proliferation efficacy for calcium deposition and ALP activity (up to 50%) for scaffolds with offset values of 50% and 100% [49]. These findings suggest that designing the architecture with different offset values can alter the cell behaviour, proliferation and differentiation.

3.4. Role of porosity in scaffold permeability

Higher permeability improves the amount of bone ingrowth and inhibits the formation of cartilaginous tissue in the regenerated site [50]. Permeability depends on porosity, orientation, size, distribution and interconnectivity of the pores. A larger pore size is preferred for cell growth and proliferation because the pores will be occluded later than smaller pores during progressive growth and will therefore provide open space for nutrient and oxygen supply and further vascularisation in newly formed bone tissues [51]. However, O'Brien et al. reduced the permeability by decreasing the pore size of collagen−GAG scaffolds *in vitro* [52]. Hence, the greatest seeding efficiency is obtained by using the smallest pore size [53]. The interconnectivity of pores must also be considered when trying to create sufficient permeability and prolong pore occlusion [54]. The interconnectivity of porous scaffolds needs to be large enough for cell infiltration. For instance, ceramic-based coralline scaffold has a pore size of 500 μm, which showed optimal cell penetration [55]. The highly open pore architecture allows the cells to pass though the length of scaffold and settle at the bottom of scaffold without binding between the cells and the surface-adsorbed proteins [56]. On the other hand, restricted pore size and lack of space for infiltration forces cells to differentiate instead of proliferation [55]. Therefore, pores with smaller dimensions may not be appropriate for encouraging bone formation

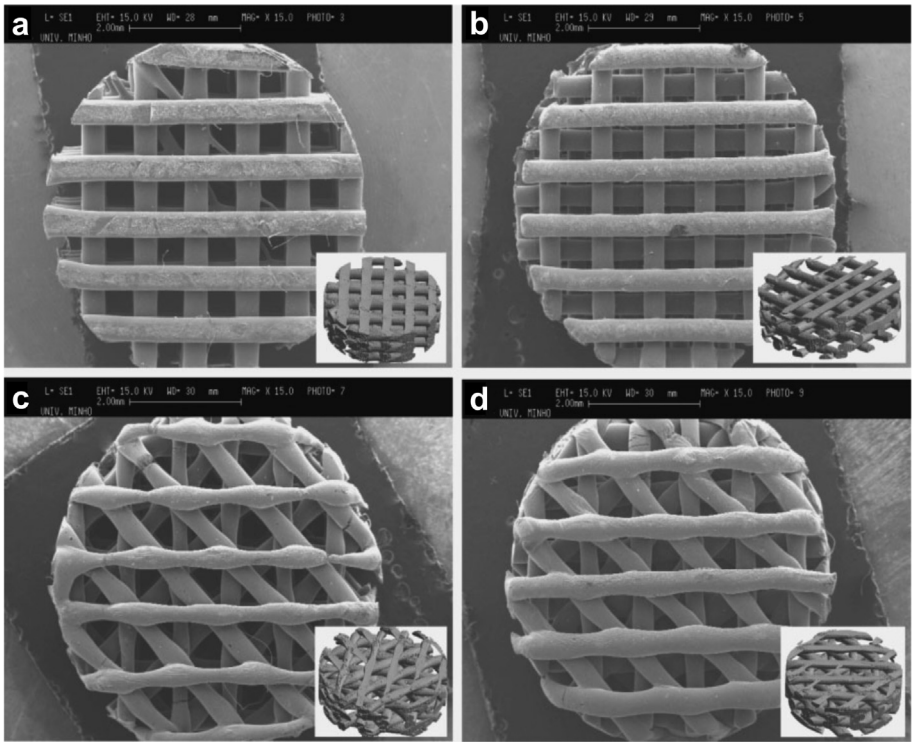

Fig. 4. SEM images of PCL scaffolds produced using a 3D plotting technique with different architecture: a) basic, b) basic-offset, c) crossed and d) crossed-offset, including μ-CT images (bars represent 2 mm). Image from Yilgor et al. [48].

because they may create a hypoxic state and stimulate chondrogenesis instead of osteogenesis [57].

3.5. Role of porosity in scaffold vascularisation

Insufficient vascularity in complex or thick tissues such as bone limits spontaneous regeneration of these parts [58]. A fracture in natural bone produces a hypoxic environment, which leads to upregulation of angiogenesis and eventually creates a vascular network [59]. This process is followed by the differentiation of (MSCs) located in the medullar cavity to cartilage [60]. The newly formed cartilage is then calcified and hardened into bone. Because of the inability of the impermeable inner cartilage to transport nutrients, the cartilage cells start to die, which creates cavities and allows the vessels to invade the cavities and the vascular mesh to develop. Osteoclasts, osteoblasts, lymphocytes and nerve cells also penetrate into the cavity, and the remaining cartilage start to collapse after secretion of osteoid by osteoblasts and osteoclasts, which form the spongy bone [61]. The hypoxic zones actuate the tips of endothelial cells, which behave like oxygen sensors and migrate toward the oxygen-deficient area. Stalk cells begin to sprout and branch to create vessel channels [62].

One strategy for creating *in vivo* preformed vessels is a two-step surgery involving implantation of a cell scaffold into a well-vascularised spot such as beneath the panniculus carnosus muscle before the next implantation at the injury site [63,64]. Another bone tissue engineering approach induces prevascularisation and osteogenesis by combining endothelial cells and osteoblasts, which will display synergistic communication and integration of VEGF, bFGF, PDGF into the biomaterials [65]. These pro-angiogenic growth factors can be supplemented within the scaffold by loading or simple coating to promote endothelial cell proliferation and vessel maturation [66]. The normal speed of neovascularisation is 1 mm per day [67]. The dual delivery of two growth factors in combination speeds the maturation of the vascular network towards full development even in larger constructs compared with single-factor delivery [68]. Multiple drug delivery requires the co-culture of two cell types that require different growth factors to proliferate and to mature into blood vessels [69]. For example, the incorporation of MSC-derived osteoblasts as the bone cells and EPCs as the blood cells which induce a greater vascular formation to support early osteogenesis [70].

Another important point for angiogenesis is the high cell density needed for vasculogenic differentiation. This in turn is a function of the size of the construct which will depend on the size of the defect. Larger constructs require a greater supply of oxygen and nutrients and if these are inadequate, spontaneous vascularisation will be insufficient and the vascular network will not penetrate into the implant [71]. The optimal pore size for vascularisation during osteogenesis was noted to be 400 μm [72]. The cell population should be adequate to cover the porous structure according to the shape and dimension of the scaffold [73].

Maintaining capillarity and providing a consistent capillary force to stimulate cell diffusion and vascularisation after implantation also needs to be considered for bone engineering. Because the macro-and microporous scaffolds which are inserted into the defect site may already be filled with biomolecules and endogenous cells from physiological fluid in the early stages of implantation, this may prevent or slow continued flow of liquid [74]. According to Rustom et al., biphasic calcium phosphate scaffolds with a micropore (<20 μm) size of 2.2 μm and macropores (>300 μm) with a size range of 650–750 μm ensures a homogeneous cell distribution and bone volume fraction throughout the scaffold via the capillarity mechanism. This study reported that the capillarity process increased the bone distribution uniformly and incorporated a variety of vascular cells in the empty dry micropores which were not occupied by submersion in fluid after implantation. This is

significant as better bone distribution improves the load-bearing of the repaired bone defect consequently [75].

The use of inorganic bioactive elements has advantages associated with their long−term activity after implantation [1]. The instability, high cost and a short half-life of growth factors *in vivo* inhibit their usefulness in clinical translation [76]. Cobalt (Co) ions are used as a cofactor for metalloproteins, which are required for the formation of the HIF-1α complex, which activates and regulates *vegf* and numerous angiogenic genes *in vitro* [77]. Zhao et al. integrated Co nanograins measuring 30−60 nm at different concentrations coated on the surface of TiO_2/TCP microporous structure with a diameter pore size of 3−4 μm. The spreading and attachment of the cells was greatly improved because of cell anchorage to the micropores of the TCP construct. Cell proliferation was best in the low Co concentration range of 10 ppm. However, a higher Co concentration (>15 ppm) caused cell cytotoxicity and reduced cell proliferation. But Co dose enhancement had positive effects on osteogenesis by increased angiogenic factors (VEGF and HIF-1a) [78]. Xu et al. reported that the release of Ca, P and Si ionic products from NAGEL, Ca7Si2P2O16 scaffolds accelerated the proliferation of human umbilical vein endothelial cells (HUVECs) in at high concentrations (12.5 mg ml^{-1}) of NAGEL extracts by promoting angiogenesis and endothelial cells for bone engineering [47].

3.6. Role of porosity in scaffold mechanical properties

There is a linear relationship between the resistance to mechanical loading and bone density or toughness [79]. The complex heterogeneous and hierarchical structure of bone tissue creates variations in compressive strength and tensile values in different regions of bone [80]. A reduction in bone mass increases the susceptibility to fracture [81]. Cortical bone contains 20% porosity along the transverse axis and has a load bearing capacity of 8−20 GPa parallel to the osteon direction. Cancellous or spongy bone (>90% porosity) is found next to joints that are highly vascular with young's modulus of 100 MPa, which is lower than that in cortical bone. Therefore, cortical bone generates compact bone which is denser than cancellous bone [82].

One effective factor for regulating the mechanical properties of a scaffold is the porosity. The mechanical properties of the scaffold tend to deplete exponentially with increasing porosity [83,84]. Cell delivery requires a highly porous scaffold (>90%), and porosity >80% is not recommended for polymeric scaffold implantation into bone defects [85,86]. The polymer molecular weight can also affect the porosity, interconnectivity, pore size and mechanical properties of a scaffold [15]. Contradictions in mechanical property results between *in vitro* and *in vivo* studies may have been affected by different cell types that desire different pore sizes for localization in the scaffold after implantation. For example, fibroblasts, which prefer to be deposited in smaller pores compared with bone cells that prefer larger pores. According to the study of Roosa et al., the mechanical properties were higher in scaffolds with pore sizes of 350 μm compared to 550 and 800 μm 4 weeks after implantation. This increase may be due to initial filling with fibroblast cells that prefer smaller pore sizes while the bone cells preferred the larger pores (550 and 800 μm). The mechanical stability of the scaffold therefore decreases over time following the addition of bone cells into the larger pores [26].

The Young's modulus and mechanical properties are affected by modification of the biomaterials. For example, calcium phosphate (CaP) scaffolds are an osteoconductive material that has been used in bone tissue engineering and influence biomaterial stiffness [87]. One of the parameters which increases the proliferation of the osteoblasts is the stiffness of the biomaterial. The submicron and nanoscale surface roughness of the pore wall promotes the differentiation and ingrowth of anchorage-dependent bone-forming cells [29]. Engler et al. confirmed that mesenchymal stem cells differentiate towards skeletal muscle and bone lineages on stiffer substrates and neural cells on softer substrates [88]. According to Gharibi et al., mechanical loading on CaP scaffolds activates transcription factors which upregulate the genes controlling osteoblast differentiation and proliferation such as *ERK1/2* and *RUNX2* and eventually augment mineralisation *in vitro* [89].

Other factors such as pore size distribution, homogeneity or heterogeneity of the pores, fibre positioning and orientation, and morphology of the pores also play an important role in determining the ultimate mechanical properties [90]. Serra et al. reported that poly (L-lactide)-b-poly (ethylene glycol) with composite CaP glass (PLA/PEG/G5) scaffolds with orthogonal structure exhibited greater compression strength than those with displaced double-layer patterns. Although the presence of glass in PLA/PEG/G5 increased the compressive modulus, the resistance to mechanical stress decreased because of the large pore sizes [91]. The construct with only one large pore size had a lower Young modulus and poorer mechanical properties [92,93].

The simple architecture of homogeneous scaffolds is prone to collapse under high stress. The complexity of non-uniform porous scaffolds allows them to recover after deformation and maintain their elastic state, which is critical for the effective use of implanted biomaterials and biomedical applications [39]. Ma et al. produced 3D biodegradable porous PLLA and PLGA scaffolds and their mechanical analysis showed that the maximum supported stress was achieved by using uniform small pores. Although heterogeneous porous patterns containing both small and large pore sizes produced better mechanical properties [94]. One study indicated better compressive strength and non-brittle failure for a porosity-graded (200−400 μm pore diameter) calcium polyphosphate (CPP) scaffold than a homogeneous porous structure (H-CPP). The reason being increased degradation in H-CPP compared with the porosity-graded CPP [95].

The orientation of pores is another parameter that directly affects the mechanical properties of scaffolds [96]. Arora et al. reported maximum mechanical properties and a doubled Young modulus for aligned pores *in vitro* and when implanted into an injury site [97]. A more complex morphological architecture has greater compressive strength [98], e.g. Young's modulus was reported as 9.81 MPa for a blended PCL/PLGA bio-scaffold with a diagonal morphology, 7.43 MPa for that with a stagger morphology, and 6.05 MPa for that with a lattice morphology [99]. Other studies by Ma et al. reported that spherical pores in a PLGA scaffold had better mechanical properties than cubic pores [94].

3.7. Role of porosity in scaffold degradation rate

The pore size plays an important role in the pattern of scaffold degradation. Although greater porosity leads to further permeability, which ultimately results in faster degradation, other parameters such as the homogeneity of pores, morphology and pore size influence the degeneration of porous biomaterials [100]. For example, Wu et al. investigated the *in vitro* degradation rate of 3D porous scaffolds composed of PLGA85/15 (poly (D,L-lactide-co-glycolide)) with a porosity of 80−95% and pore size of 50−450 μm in PBS at 37 °C for 26 weeks. The scaffolds with larger pore size and lower porosity degraded faster than those with smaller pore size and higher porosity. This finding was attributed to the effect of the higher surface area in the scaffolds with larger pore size which increased the diffusion of acidic degradation products during the incubation period and led to a stronger acid-catalysed hydrolysis [101].

Pore size and porosity regulate the rate of degradation in PLA scaffolds with a pore size of 0–500 μm from solid to highly porous scaffolds with porosity >90%. In another study, degradation occurred faster in scaffolds with a larger pore size and in solid films because the degradation products were trapped in isolated pores as a result of autocatalysed degradation. Intermediate degradation behaviour was observed in scaffolds with pore sizes between 0 and 500 μm [102]. The study of Xu et al. reported that among the different pore morphologies, the square pore provided a faster degradability and scaffold weight loss [47].

4. Conclusion

This review examined the importance of pore size and porosity on cell behaviour during ossification and angiogenesis, as well as how the porosity of biomaterial scaffolds determines their mechanical and degradation properties. Among the various manufacturing techniques, additive manufacturing technologies have proved more successful in fabricating 3D custom-designed scaffolds with the best configuration to control the pore size. Macroporous (100 and 600 μm) scaffolds allow better integration with the host bone tissue, subsequent vascularisation and bone distribution. Increasing the pore size increases the permeability, which increases bone ingrowth, but small pores are more suitable for soft tissue ingrowth. Regarding the geometry of the structure, triangular, rectangular and elliptic pores support angiogenesis and cause faster cell migration because of the greater curvature while staggered and offset pores help to produce a larger bone volume compared with scaffolds with aligned patterns. The combination and ratio of endothelial cells and osteoblasts also plays a pivotal role in pre-vascularisation during osteogenesis and homogeneous bone distribution in macroporous scaffolds.

With respect to the scaffold's mechanical properties, a greater compressive modulus is associated with smaller pore sizes, a gradient porosity and staggered orientated pores. The major advantage of using gradient porosity scaffolds is their ability to maintain and recover their elastic properties after deformation, while square pores help to improve the stable mechanical strength. A faster degradation rate is attributed to a larger pore size because of the greater dispersal of acidic products during degradation.

Although several reports have shown the effects of pore size, shape and porosity on ossification, some have reported on the influence of heterogeneous porosity on degradation, mechanical properties and angiogenesis after implantation to stimulate bone healing. As a consequence, there is an extensive scope for further research in this field of bone tissue engineering.

Declaration of Competing Interest

The authors declare that they have no known competing financial interests or personal relationships that could have appeared to influence the work reported in this paper.

Acknowledgments

This study is part of PhD research project of Naghmeh Abbasi being sponsored by a scholarship from Griffith University, Australia. The authors would like to express their gratitude to the Australian Dental Research Foundation (ADRF) research grant and Dentistry and Oral Health (DOH) research grant of Griffith University supported this study.

References

[1] G.F. de Grado, L. Keller, Y. Idoux-Gillet, Q. Wagner, A.M. Musset, N. Benkirane-Jessel, F. Bornert, D. Offner, Bone substitutes: a review of their characteristics, clinical use, and perspectives for large bone defects management, J. Tissue Eng. 9 (2018), https://doi.org/10.1177/2041731418776819.
[2] S. Talebian, M. Mehrali, N. Taebnia, C.P. Pennisi, F.B. Kadumudi, J. Foroughi, M. Hasany, M. Nikkhah, M. Akbari, G. Orive, A. Dolatshahi-Pirouz, Self-healing hydrogels: the next paradigm shift in tissue engineering? Adv. Sci. 6 (16) (2019) https://doi.org/10.1002/advs.201801664.
[3] A. Oryan, S. Alidadi, A. Moshiri, N. Maffulli, Bone regenerative medicine: classic options, novel strategies, and future directions, J. Orthop. Surg. Res. 9 (2014), https://doi.org/10.1186/1749-799X-9-18.
[4] R. Owen, G.C. Reilly, In vitro models of bone remodelling and associated disorders, Front Bioeng. Biotechnol. 6 (2018), https://doi.org/10.3389/fbioe.2018.00134.
[5] Y. Efraim, B. Schoen, S. Zahran, T. Davidov, G. Vasilyev, L. Baruch, E. Zussman, M. Machluf, 3D structure and processing methods direct the biological attributes of ECM-based cardiac scaffolds, Sci Rep-Uk 9 (2019), https://doi.org/10.1038/s41598-019-41831-9.
[6] S. Limmahakhun, A. Oloyede, K. Sitthiseripratip, Y. Xiao, C. Yan, 3D-printed cellular structures for bone biomimetic implants, Addit. Manuf. 15 (2017) 93–101.
[7] T.B. Wissing, V. Bonito, C.V.C. Bouten, A.I.P.M. Smits, Biomaterial-driven in situ cardiovascular tissue engineering-a multi-disciplinary perspective, Npj Regen. Med. 2 (2017), https://doi.org/10.1016/j.addma.2017.03.010.
[8] A. Kashirina, Y.T. Yao, Y.J. Liu, J.S. Leng, Biopolymers as bone substitutes: a review, Biomater. Sci.-Uk 7 (10) (2019) 3961–3983, https://doi.org/10.1039/c9bm00664h.
[9] A. Saberi, F. Jabbari, P. Zarrintaj, M.R. Saeb, M. Mozafari, Electrically conductive materials: opportunities and challenges in tissue engineering, Biomolecules 9 (9) (2019), https://doi.org/10.3390/biom9090448.
[10] T.L. Jenkins, D. Little, Synthetic scaffolds for musculoskeletal tissue engineering: cellular responses to fiber parameters, Npj Regen. Med. 4 (2019), https://doi.org/10.1038/s41536-019-0076-5.
[11] M. Mehrasa, M.A. Asadollahi, B. Nasri-Nasrabadi, K. Ghaedi, H. Salehi, A. Dolatshahi-Pirouz, A. Arpanaei, Incorporation of mesoporous silica nanoparticles into random electrospun PLGA and PLGA/gelatin nanofibrous scaffolds enhances mechanical and cell proliferation properties, Mater. Sci. Eng. C Mater Biol. Appl. 66 (2016) 25–32, https://doi.org/10.1016/j.msec.2016.04.031.
[12] A. Eltom, G.Y. Zhong, A. Muhammad, Scaffold techniques and designs in tissue engineering functions and purposes: a review, Ann. Mater. Sci. Eng. (2019), https://doi.org/10.1155/2019/3429527.
[13] N. Bodenberger, D. Kubiczek, I. Abrosimova, A. Scharm, F. Kipper, P. Walther, F. Rosenau, Evaluation of methods for pore generation and their influence on physio-chemical properties of a protein based hydrogel, Biotechnol. Rep. (Amst) 12 (2016) 6–12, https://doi.org/10.1016/j.btre.2016.09.001.
[14] K. Kosowska, M. Henczka, The influence of supercritical foaming conditions on properties of polymer scaffolds for tissue engineering, Chem. Process Eng-Inz 38 (4) (2017) 535–541, https://doi.org/10.1515/cpe-2017-0042.
[15] E. Babaie, S.B. Bhaduri, Fabrication aspects of porous biomaterials in orthopedic applications: a review, ACS Biomater. Sci. Eng. 4 (1) (2018) 1–39, https://doi.org/10.1021/acsbiomaterials.7b00615.
[16] R. Scaffaro, F. Lopresti, A. Maio, F. Sutera, L. Botta, Development of polymeric functionally graded scaffolds: a brief review, J. Appl. Biomater. Func. 15 (2) (2017) E107–E121, https://doi.org/10.5301/jabfm.5000332.
[17] A. Hamed, N. Shehata, M. Elosairy, Investigation of conical spinneret in generating more dense and compact electrospun nanofibers, Polymers-Basel 10 (1) (2018), https://doi.org/10.3390/polym10010012.
[18] F.U. Din, W. Aman, I. Ullah, O.S. Qureshi, O. Mustapha, S. Shafique, A. Zeb, Effective use of nanocarriers as drug delivery systems for the treatment of selected tumors, Int. J. Nanomed. 12 (2017) 7291–7309, https://doi.org/10.2147/Ijn.S146315.
[19] S. Zaiss, T.D. Brown, J.C. Reichert, A. Berner, Poly(epsilon-caprolactone) scaffolds fabricated by melt electrospinning for bone tissue engineering, Materials 9 (4) (2016), https://doi.org/10.3390/ma9040232.
[20] N. Abbasi, A. Abdal-hay, S. Hamlet, E. Graham, S. Ivanovski, Effects of gradient and offset architectures on the mechanical and biological properties of 3-D melt electrowritten (MEW) scaffolds, ACS Biomater. Sci. Eng. 5 (7) (2019) 3448–3461, https://doi.org/10.1021/acsbiomaterials.8b01456.
[21] F.S.L. Bobbert, A.A. Zadpoor, Effects of bone substitute architecture and surface properties on cell response, angiogenesis, and structure of new bone, J. Mater. Chem. B 5 (31) (2017) 6175–6192, https://doi.org/10.1039/c7tb00741h.
[22] S. Mohammadzadehmoghadam, Y. Dong, I.J. Davies, Modeling electrospun nanofibers: an overview from theoretical, empirical, and numerical approaches, Int. J. Polym. Mater. 65 (17) (2016) 901–915, https://doi.org/10.1080/00914037.2016.1180617.
[23] Y. Sugawara, H. Kamioka, T. Honjo, K. Tezuka, T. Takano-Yamamoto, Three-dimensional reconstruction of chick calvarial osteocytes and their cell processes using confocal microscopy, Bone 36 (5) (2005) 877–883, https://doi.org/10.1016/j.bone.2004.10.008.

[24] G. Iviglia, S. Kargozar, F. Baino, Biomaterials, current strategies, and novel nano-technological approaches for periodontal regeneration, J. Funct. Biomater. 10 (1) (2019), https://doi.org/10.3390/jfb10010003.
[25] J. Liu, G. Chen, H. Xu, K. Hu, J.F. Sun, M. Liu, F.M. Zhang, N. Gu, Pre-vascularization in fibrin Gel/PLGA microsphere scaffolds designed for bone regeneration, NPG Asia Mater. 10 (2018) 827–839, https://doi.org/10.1038/s41427-018-0076-8.
[26] S.M.M. Roosa, J.M. Kemppainen, E.N. Moffitt, P.H. Krebsbach, S.J. Hollister, The pore size of polycaprolactone scaffolds has limited influence on bone regeneration in an in vivo model, J. Biomed. Mater. Res. 92a (1) (2010) 359–368, https://doi.org/10.1002/jbm.a.32381.
[27] M.Q. Cheng, T.E.H.J. Wahafu, G.F. Jiang, W. Liu, Y.Q. Qiao, X.C. Peng, T. Cheng, X.L. Zhang, G. He, X.Y. Liu, A novel open-porous magnesium scaffold with controllable microstructures and properties for bone regeneration, Sci Rep-Uk 6 (2016), https://doi.org/10.1038/srep24134.
[28] T.C. Lim, K.S. Chian, K.F. Leong, Cryogenic prototyping of chitosan scaffolds with controlled micro and macro architecture and their effect on in vivo neovascularization and cellular infiltration, J. Biomed. Mater. Res. 94a (4) (2010) 1303–1311, https://doi.org/10.1002/jbm.a.32747.
[29] X.N. Chen, H.Y. Fan, X.W. Deng, L.N. Wu, T. Yi, L.X. Gu, C.C. Zhou, Y.J. Fan, X.D. Zhang, Scaffold structural microenvironmental cues to guide tissue regeneration in bone tissue applications, Nanomaterials-Basel 8 (11) (2018), https://doi.org/10.3390/nano8110960.
[30] S. Bianco, D. Mancardi, A. Merlino, B. Bussolati, L. Munaron, Hypoxia and hydrogen sulfide differentially affect normal and tumor-derived vascular endothelium, Redox Biol. 12 (2017) 499–504, https://doi.org/10.1016/j.redox.2017.03.015.
[31] S. Mukherjee, S. Darzi, K. Paul, J.A. Werkmeister, C.E. Gargett, Mesenchymal stem cell-based bioengineered constructs: foreign body response, cross-talk with macrophages and impact of biomaterial design strategies for pelvic floor disorders, Interface Focus 9 (4) (2019), https://doi.org/10.1098/rsfs.2018.0089.
[32] C.M. Murphy, F.J. O'Brien, Understanding the effect of mean pore size on cell activity in collagen-glycosaminoglycan scaffolds, Cell Adhes. Migrat. 4 (3) (2010) 377–381, https://doi.org/10.4161/cam.4.3.11747.
[33] C.M. Murphy, M.G. Haugh, F.J. O'Brien, The effect of mean pore size on cell attachment, proliferation and migration in collagen-glycosaminoglycan scaffolds for bone tissue engineering, Biomaterials 31 (3) (2010) 461–466, https://doi.org/10.1016/j.biomaterials.2009.09.063.
[34] L. Morejon, J.A. Delgado, A.A. Ribeiro, M.V. de Oliveira, E. Mendizabal, I. Garcia, A. Alfonso, P. Poh, M. van Griensven, E.R. Balmayor, Development, characterization and in vitro biological properties of scaffolds fabricated from calcium phosphate nanoparticles, Int. J. Mol. Sci. 20 (7) (2019), https://doi.org/10.3390/ijms20071790.
[35] P. Diaz-Rodriguez, M. Sanchez, M. Landin, Drug-loaded biomimetic ceramics for tissue engineering, Pharmaceutics 10 (4) (2018), https://doi.org/10.3390/pharmaceutics10040272.
[36] S.J. Estermann, S. Scheiner, Multiscale modeling provides differentiated insights to fluid flow-driven stimulation of bone cellular activities, Front. Physiol. 6 (2018), https://doi.org/10.3389/fphy.2018.00076.
[37] A. Boccaccio, A.E. Uva, M. Fiorentino, G. Mori, G. Monno, Geometry design optimization of functionally graded scaffolds for bone tissue engineering: a mechanobiological approach, PloS One 11 (1) (2016), https://doi.org/10.1371/journal.pone.0146935.
[38] A. Di Luca, B. Ostrowska, I. Lorenzo-Moldero, A. Lepedda, W. Swieszkowski, C. Van Blitterswijk, L. Moroni, Gradients in pore size enhance the osteogenic differentiation of human mesenchymal stromal cells in three-dimensional scaffolds, Sci. Rep. 6 (2016) 22898, https://doi.org/10.1038/srep22898.
[39] J.M. Sobral, S.G. Caridade, R.A. Sousa, J.F. Mano, R.L. Reis, Three-dimensional plotted scaffolds with controlled pore size gradients: effect of scaffold geometry on mechanical performance and cell seeding efficiency, Acta Biomater. 7 (3) (2011) 1009–1018, https://doi.org/10.1016/j.actbio.2010.11.003.
[40] A. Boccaccio, A.E. Uva, M. Fiorentino, L. Lamberti, G. Monno, A mechanobiology-based algorithm to optimize the microstructure geometry of bone tissue scaffolds, Int. J. Biol. Sci. 12 (1) (2016) 1–17, https://doi.org/10.7150/ijbs.13158.
[41] S. Pina, V.P. Ribeiro, C.F. Marques, F.R. Maia, T.H. Silva, R.L. Reis, J.M. Oliveira, Scaffolding strategies for tissue engineering and regenerative medicine applications, Materials 12 (11) (2019), https://doi.org/10.3390/ma12111824.
[42] J. Knychala, N. Bouropoulos, C.J. Catt, O.L. Katsamenis, C.P. Please, B.G. Sengers, Pore geometry regulates early stage human bone marrow cell tissue formation and organisation, Ann. Biomed. Eng. 41 (5) (2013) 917–930, https://doi.org/10.1007/s10439-013-0748-z.
[43] M. Bianchi, E.R.U. Edreira, J.G.C. Wolke, Z.T. Birgani, P. Habibovic, J.A. Jansen, A. Tampieri, M. Marcacci, S.C.G. Leeuwenburgh, J.J.J.P. van den Beucken, Substrate geometry directs the in vitro mineralization of calcium phosphate ceramics, Acta Biomater. 10 (2) (2014) 661–669, https://doi.org/10.1016/j.actbio.2013.10.026.
[44] P. Chocholata, V. Kulda, V. Babuska, Fabrication of scaffolds for bone-tissue regeneration, Materials 12 (4) (2019), https://doi.org/10.3390/ma12040568.
[45] S.A. Redey, S. Razzouk, C. Rey, D. Bernache-Assollant, G. Leroy, M. Nardin, G. Cournot, Osteoclast adhesion and activity on synthetic hydroxyapatite, carbonated hydroxyapatite, and natural calcium carbonate: relationship to surface energies, J. Biomed. Mater. Res. 45 (2) (1999) 140–147, https://doi.org/10.1002/(sici)1097-4636(199905)45:2<140::aid-jbm9>3.0.co;2-i.
[46] S. Van Bael, Y.C. Chai, S. Truscello, M. Moesen, G. Kerckhofs, H. Van Oosterwyck, I.P. Kruth, J. Schrooten, The effect of pore geometry on the in vitro biological behavior of human periosteum-derived cells seeded on selective laser-melted Ti6Al4V bone scaffolds, Acta Biomater. 8 (7) (2012) 2824–2834, https://doi.org/10.1016/j.actbio.2012.04.001.
[47] M.C. Xu, D. Zhai, J. Chang, C.T. Wu, In vitro assessment of three-dimensionally plotted nagelschmidtite bioceramic scaffolds with varied macropore morphologies, Acta Biomater. 10 (1) (2014) 463–476, https://doi.org/10.1016/j.actbio.2013.09.011.
[48] P. Yilgor, R.A. Sousa, R.L. Reis, N. Hasirci, V. Hasirci, 3D plotted PCL scaffolds for stem cell based bone tissue engineering, Macromol. Symp. 269 (2008) 92–99, https://doi.org/10.1002/masy.200850911.
[49] M. Yeo, C.G. Simon, G. Kim, Effects of offset values of solid freeform fabricated PCL-beta-TCP scaffolds on mechanical properties and cellular activities in bone tissue regeneration, J. Mater. Chem. 22 (40) (2012) 21636–21646, https://doi.org/10.1039/c2jm31165h.
[50] G. Turnbull, J. Clarke, F. Picard, P. Riches, L.L. Jia, F.X. Han, B. Li, W.M. Shu, 3D bioactive composite scaffolds for bone tissue engineering, Bioact. Mater 3 (3) (2018) 278–314, https://doi.org/10.1016/j.bioactmat.2017.10.001.
[51] Y.Q. Kang, J. Chang, Channels in a porous scaffold: a new player for vascularization, Regen. Med. 13 (6) (2018) 704–715, https://doi.org/10.2217/rme-2018-0022.
[52] F.J. O'Brien, B.A. Harley, I.V. Yannas, L.J. Gibson, The effect of pore size on cell adhesion in collagen-GAG scaffolds, Biomaterials 26 (4) (2005) 433–441, https://doi.org/10.1016/j.biomaterials.2004.02.052.
[53] B. Wysocki, J. Idaszek, K. Szlazak, K. Strzelczyk, T. Brynk, K.J. Kurzydlowski, W. Swieszkowski, Post processing and biological evaluation of the titanium scaffolds for bone tissue engineering, Materials 9 (3) (2016), https://doi.org/10.3390/ma9030197.
[54] Q.C. Ran, W.H. Yang, Y. Hu, X.K. She, Y.L. Yu, Y. Xiang, K.Y. Cai, Osteogenesis of 3D printed porous Ti6Al4V implants with different pore sizes, J. Mech. Behav. Biomed. 84 (2018) 1–11, https://doi.org/10.1016/j.jmbbm.2018.04.010.
[55] C. Vitale-Brovarone, F. Baino, M. Miola, R. Mortera, B. Onida, E. Verne, Glass-ceramic scaffolds containing silica mesophases for bone grafting and drug delivery, J. Mater. Sci. Mater. Med. 20 (3) (2009) 809–820, https://doi.org/10.1007/s10856-008-3635-7.
[56] Z.M. Wang, Z.F. Wang, W.W. Lu, W.X. Zhen, D.Z. Yang, S.L. Peng, Novel biomaterial strategies for controlled growth factor delivery for biomedical applications, NPG Asia Mater. 9 (2017), https://doi.org/10.1038/am.2017.171.
[57] T.H. Lin, H.C. Wang, W.H. Cheng, H.C. Hsu, M.L. Yeh, Osteochondral tissue regeneration using a tyramine-modified bilayered PLGA scaffold combined with articular chondrocytes in a porcine model, Int. J. Mol. Sci. 20 (2) (2019), https://doi.org/10.3390/ijms20020326.
[58] M. Dang, L. Saunders, X.F. Niu, Y.B. Fan, P.X. Ma, Biomimetic delivery of signals for bone tissue engineering, Bone Res. 6 (2018), https://doi.org/10.1038/s41413-018-0025-8.
[59] K.K. Sivaraj, R.H. Adams, Blood vessel formation and function in bone, Development 143 (15) (2016) 2706–2715, https://doi.org/10.1242/dev.136861.
[60] P.H. Su, Y. Tian, C.F. Yang, X.L. Ma, X. Wang, J.W. Pei, A.R. Qian, Mesenchymal stem cell migration during bone formation and bone diseases therapy, Int. J. Mol. Sci. 19 (8) (2018), https://doi.org/10.3390/ijms19082343.
[61] G. Breeland, R.G. Menezes, Embryology, Bone Ossification, StatPearls, Treasure Island (FL), 2019. PMID: 30969540.
[62] K. Hu, B.R. Olsen, Vascular endothelial growth factor control mechanisms in skeletal growth and repair, Dev. Dynam. 246 (4) (2017) 227–234, https://doi.org/10.1002/dvdy.24463.
[63] U. Kneser, E. Polykandriotis, J. Ohnolz, K. Heidner, L. Grabinger, S. Euler, K.U. Amann, A. Hess, K. Brune, P. Greil, M. Sturzl, R.E. Horch, Engineering of vascularized transplantable bone tissues: induction of axial vascularization in an osteoconductive matrix using an arteriovenous loop, Tissue Eng. 12 (7) (2006) 1721–1731, https://doi.org/10.1089/ten.2006.12.1721.
[64] P.H. Warnke, I.N.G. Springer, J. Wiltfang, Y. Acil, H. Eufinger, M. Wehmoller, P.A.J. Russo, H. Bolte, E. Sherry, E. Behrens, H. Terheyden, Growth and transplantation of a custom vascularised bone graft in a man, Lancet 364 (9436) (2004) 766–770, https://doi.org/10.1016/S0140-6736(04)16935-3.
[65] R.J. Kant, K.L.K. Coulombe, Integrated approaches to spatiotemporally directing angiogenesis in host and engineered tissues, Acta Biomater. 69 (2018) 42–62, https://doi.org/10.1016/j.actbio.2018.01.017.
[66] S. Saberianpour, M. Heidarzadeh, M.H. Geranmayeh, H. Hosseinkhani, R. Rahbarghazi, M. Nouri, Tissue engineering strategies for the induction of angiogenesis using biomaterials, J. Biol. Eng. 12 (2018), https://doi.org/10.1186/s13036-018-0133-4.
[67] H. Eckardt, M. Ding, M. Lind, E.S. Hansen, K.S. Christensen, I. Hvid, Recombinant human vascular endothelial growth factor enhances bone healing in an experimental nonunion model, J. Bone Jt. Surg. Br. 87b (10) (2005) 1434–1438, https://doi.org/10.1302/0301-620X.87B10.16226.
[68] J. Jiang, S.H. Wang, F. Chai, C.C. Ai, S.Y. Chen, The study on vascularisation and osteogenesis of BMP/VEGF co-modified tissue engineering bone in vivo, RSC Adv. 6 (48) (2016) 41800–41808, https://doi.org/10.1039/c6ra03111k.
[69] Y.M. Kook, Y. Jeong, K. Lee, W.G. Koh, Design of biomimetic cellular scaffolds for co-culture system and their application, J. Tissue Eng. 8 (2017), https://doi.org/10.1177/2041731417724640.

[70] A.R. Amini, T.O. Xu, R.M. Chidambaram, S.P. Nukavarapu, Oxygen tension-controlled matrices with osteogenic and vasculogenic cells for vascularized bone regeneration in vivo, Tissue Eng. Pt A 22 (7–8) (2016) 610–620, https://doi.org/10.1089/ten.tea.2015.0310.
[71] C. Tomasina, T. Bodet, C. Mota, L. Moroni, S. Camarero-Espinosa, Bioprinting vasculature: materials, cells and emergent techniques, Materials 12 (17) (2019), https://doi.org/10.3390/ma12172701.
[72] L. Li, Y.X. Li, L.F. Yang, F. Yu, K.J. Zhang, J. Jin, J.P. Shi, L.Y. Zhu, H.X. Liang, X.S. Wang, Q. Jiang, Polydopamine coating promotes early osteogenesis in 3D printing porous Ti6Al4V scaffolds, Ann. Transl. Med. 7 (11) (2019), https://doi.org/10.21037/atm.2019.04.79.
[73] A.S. Neto, J.M.F. Ferreira, Synthetic and marine-derived porous scaffolds for bone tissue engineering, Materials 11 (9) (2018), https://doi.org/10.3390/ma11091702.
[74] K. Zhang, Y.B. Fan, N. Dunne, X.M. Li, Effect of microporosity on scaffolds for bone tissue engineering, Regen. Biomater. 5 (2) (2018) 115–124, https://doi.org/10.1093/rb/rby001.
[75] L.E. Rustom, T. Boudou, S.Y. Lou, I. Pignot-Paintrand, B.W. Nemke, Y. Lu, M.D. Markel, C. Picart, A.W. Johnson, Micropore-induced capillarity enhances bone distribution in vivo in biphasic calcium phosphate scaffolds, Acta Biomater. 44 (2016) 144–154, https://doi.org/10.1016/j.actbio.2016.08.025.
[76] D. Tang, R.S. Tare, L.Y. Yang, D.F. Williams, K.L. Ou, R.O. Oreffo, Biofabrication of bone tissue: approaches, challenges and translation for bone regeneration, Biomaterials 83 (2016) 363–382, https://doi.org/10.1016/j.biomaterials.2016.01.024.
[77] J.H. Zhou, L.Z. Zhao, Hypoxia-mimicking Co doped TiO2 microporous coating on titanium with enhanced angiogenic and osteogenic activities, Acta Biomater. 43 (2016) 358–368, https://doi.org/10.1016/j.actbio.2016.07.045.
[78] F. Zhao, Y.J. Yin, W.W. Lu, J.C. Leong, W.J. Zhang, J.Y. Zhang, M.F. Zhang, K.D. Yao, Preparation and histological evaluation of biomimetic three-dimensional hydroxyapatite/chitosan-gelatin network composite scaffolds, Biomaterials 23 (15) (2002) 3227–3234, https://doi.org/10.1016/S0142-9612(02)00077-7.
[79] N. Eliaz, N. Metoki, Calcium phosphate bioceramics: a review of their history, structure, properties, coating technologies and biomedical applications, Materials 10 (4) (2017), https://doi.org/10.3390/ma10040334.
[80] E.F. Morgan, G.U. Unnikrisnan, A.I. Hussein, Bone mechanical properties in healthy and diseased states, Annu. Rev. Biomed. Eng. 20 (2018) 119–143, https://doi.org/10.1146/annurev-bioeng-062117-121139.
[81] T. Sozen, L. Ozisik, N.C. Basaran, An overview and management of osteoporosis, Eur. J. Rheumatol. 4 (1) (2017) 46–56, https://doi.org/10.5152/eurjrheum.2016.048.
[82] R. Setiawati, D.N. Utomo, F.A. Rantam, N.N. Ifran, N.C. Budhiparama, Early graft tunnel healing after anterior cruciate ligament reconstruction with intratunnel injection of bone marrow mesenchymal stem cells and vascular endothelial growth factor, Orthop. J. Sports Med. 5 (6) (2017), https://doi.org/10.1177/2325967117708548.
[83] S.J. Hollister, Porous scaffold design for tissue engineering, Nat. Mater. 4 (7) (2005) 518–524, https://doi.org/10.1038/nmat1421.
[84] F. Afghah, C. Dikyol, M. Altunbek, B. Koc, Biomimicry in bio-manufacturing: developments in melt electrospinning writing technology towards hybrid biomanufacturing, Appl. Sci.-Basel 9 (17) (2019), https://doi.org/10.3390/app9173540.
[85] B.G. Sengers, C.P. Please, M. Taylor, R.O.C. Oreffo, Experimental-computational evaluation of human bone marrow stromal cell spreading on trabecular bone structures, Ann. Biomed. Eng. 37 (6) (2009) 1165–1176, https://doi.org/10.1007/s10439-009-9676-3.
[86] M.Y. Liu, Y.G. Lv, Reconstructing bone with natural bone graft: a review of in vivo studies in bone defect animal model, Nanomaterials-Basel 8 (12) (2018), https://doi.org/10.3390/nano8120999.
[87] A. Bigi, E. Boanini, Functionalized biomimetic calcium phosphates for bone tissue repair, J. Appl. Biomater. Func. 15 (4) (2017) E313–E325, https://doi.org/10.5301/jabfm.5000367.
[88] A.J. Engler, S. Sen, H.L. Sweeney, D.E. Discher, Matrix elasticity directs stem cell lineage specification, Cell 126 (4) (2006) 677–689, https://doi.org/10.1016/j.cell.2006.06.044.
[89] B. Gharibi, G. Cama, M. Capurro, I. Thompson, S. Deb, L. Di Silvio, F.J. Hughes, Gene expression responses to mechanical stimulation of mesenchymal stem cells seeded on calcium phosphate cement, Tissue Eng Pt. A 19 (21–22) (2013) 2426–2438, https://doi.org/10.1089/ten.tea.2012.0623.
[90] A.K. Gaharwar, L.M. Cross, C.W. Peak, K. Gold, J.K. Carrow, A. Brokesh, K.A. Singh, 2D nanoclay for biomedical applications: regenerative medicine, therapeutic delivery, and additive manufacturing, Adv. Mater. 31 (23) (2019), e1900332, https://doi.org/10.1002/adma.201900332.
[91] T. Serra, J.A. Planell, M. Navarro, High-resolution PLA-based composite scaffolds via 3-D printing technology, Acta Biomater. 9 (3) (2013) 5521–5530, https://doi.org/10.1016/j.actbio.2012.10.041.
[92] Q.R. Xiong, T.G. Baychev, A.P. Jivkov, Review of pore network modelling of porous media: experimental characterisations, network constructions and applications to reactive transport, J. Contam. Hydrol. 192 (2016) 101–117, https://doi.org/10.1016/j.jconhyd.2016.07.002.
[93] S. Zhao, J.X. Zhao, G.Z. Han, Advances in the study of mechanical properties and constitutive law in the field of wood research, Iop Conf. Ser-Mat Sci. 137 (2016), https://doi.org/10.1088/1757-899x/137/1/012036.
[94] P.X. Ma, J.W. Choi, Biodegradable polymer scaffolds with well-defined interconnected spherical pore network, Tissue Eng. 7 (1) (2001) 23–33, https://doi.org/10.1089/107632701300003269.
[95] Q.B. Wang, Q.G. Wang, C.X. Wan, Preparation and evaluation of a biomimetic scaffold with porosity gradients in vitro, An. Acad. Bras. Cienc. 84 (1) (2012) 9–16, https://doi.org/10.1590/S0001-37652012000100003.
[96] M.A. Velasco, Y. Lancheros, D.A. Garzon-Alvarado, Geometric and mechanical properties evaluation of scaffolds for bone tissue applications designing by a reaction-diffusion models and manufactured with a material jetting system, J. Comput. Des. Eng. 3 (4) (2016) 385–397, https://doi.org/10.1016/j.jcde.2016.06.006.
[97] A. Arora, A. Kothari, D.S. Katti, Pore orientation mediated control of mechanical behavior of scaffolds and its application in cartilage-mimetic scaffold design, J. Mech. Behav. Biomed. Mater. 51 (2015) 169–183, https://doi.org/10.1016/j.jmbbm.2015.06.033.
[98] M. Vetrik, M. Parizek, D. Hadraba, O. Kukackova, J. Brus, H. Hlidkova, L. Komankova, J. Hodan, O. Sedlacek, M. Slouf, L. Bacakova, M. Hruby, Porous heat-treated polyacrylonitrile scaffolds for bone tissue engineering, ACS. Appl. Mater. Interfaces 10 (10) (2018) 8496–8506, https://doi.org/10.1021/acsami.7b18839.
[99] J.S. Lee, H.D. Cha, J.H. Shim, J.W. Jung, J.Y. Kim, D.W. Cho, Effect of pore architecture and stacking direction on mechanical properties of solid freeform fabrication-based scaffold for bone tissue engineering, J. Biomed. Mater. Res. 100 (7) (2012) 1846–1853, https://doi.org/10.1002/jbm.a.34149.
[100] L. Qin, C. Zhai, S.M. Liu, J.Z. Xu, Factors controlling the mechanical properties degradation and permeability of coal subjected to liquid nitrogen freeze-thaw, Sci Rep-Uk 7 (2017), https://doi.org/10.1038/s41598-017-04019-7.
[101] L.B. Wu, J.D. Ding, Effects of porosity and pore size on in vitro degradation of three-dimensional porous poly(D,L-lactide-co-glycolide) scaffolds for tissue engineering, J. Biomed. Mater. Res. 75a (4) (2005) 767–777, https://doi.org/10.1002/jbm.a.30487.
[102] E. Diaz, I. Puerto, S. Ribeiro, S. Lanceros-Mendez, J.M. Barandiarian, The influence of copolymer composition on PLGA/nHA scaffolds' cytotoxicity and in vitro degradation, Nanomaterials-Basel 7 (7) (2017), https://doi.org/10.3390/nano7070173.